◆ Human Brain Mapping 35:5093–5105 (2014) ◆

Impact of Chiasma Opticum Malformations on the Organization of the Human Ventral Visual Cortex

**Falko R. Kaule,[1,2] Barbara Wolynski,[1] Irene Gottlob,[3] Joerg Stadler,[4] Oliver Speck,[4,5,6] Martin Kanowski,[7] Synke Meltendorf,[1] Wolfgang Behrens-Baumann,[1] and Michael B. Hoffmann[1,6]*

[1]*Department of Ophthalmology, Visual Processing Laboratory, Otto-von-Guericke University, Magdeburg, Germany*
[2]*Department of Experimental Psychology, Otto-von-Guericke University, Universitätsplatz 2, Magdeburg, Germany*
[3]*Ophthalmology Group, University of Leicester, Leicester Royal Infirmary, Robert Kilpatrick Clinical Sciences Building, Leicester, United Kingdom*
[4]*Leibniz Institute for Neurobiology, Brenneckestraße 6, Magdeburg, Germany*
[5]*Department Biomedical Magnetic Resonance, Institute for Experimental Physics, Otto-von-Guericke University Magdeburg, Magdeburg, Germany*
[6]*Center for Behavioral Brain Sciences, Magdeburg, Germany*
[7]*Department of Neurology, Otto-von-Guericke University, Magdeburg, Germany*

Abstract: Congenital malformations of the optic chiasm, such as enhanced and reduced crossing of the optic nerve fibers, are evident in albinism and achiasma, respectively. In early visual cortex the resulting additional visual input from the ipsilateral visual hemifield is superimposed onto the normal retinotopic representation of the contralateral visual field, which is likely due to conservative geniculostriate projections. Counterintuitively, this organization in early visual cortex does not have profound consequences on visual function. Here we ask, whether higher stages of visual processing provide a correction to the abnormal representation allowing for largely normal perception. To this end we assessed the organization patterns of early and ventral visual cortex in five albinotic, one achiasmic, and five control participants. In albinism and achiasma the mirror-symmetrical superposition of the ipsilateral and contalateral visual fields was evident not only in early visual cortex, but also in the higher areas of the ventral processing stream. Specifically, in the visual areas VO1/2 and PHC1/2 no differences in the extent, the degree of superposition, and the magnitude of the responses were evident in comparison to the early visual areas. Consequently, the highly atypical organization of the primary visual cortex was propagated downstream to highly specialized processing stages in an undiminished and unchanged manner. This indicates largely unaltered cortico-cortical connections in both types of

Funded by: German Research Foundation (DFG), Grant number: HO-2002/10-1; Federal State of Saxony-Anhalt, Project: Center for Behavioral Brain Sciences (CBBS).

*Correspondence to: Michael B. Hoffmann, Department of Ophthalmology, Otto-von-Guericke-University, Leipziger Str. 44, 39120 Magdeburg. E-mail: michael.hoffmann@med.ovgu.de

Received for publication 29 October 2013; Revised 21 February 2014; Accepted 4 April 2014.

DOI: 10.1002/hbm.22534

Published online 25 April 2014 in Wiley Online Library (wileyonlinelibrary.com).

misrouting, i.e., enhanced and reduced crossing of the optic nerves. It is concluded that main aspects of visual function are preserved despite sizable representation abnormalities in the ventral visual processing stream. *Hum Brain Mapp 35:5093–5105, 2014.*

Key words: albino; achiasmia; decussation; chiasm; visual cortex; visual areas; retinotopic mapping; fMRI

INTRODUCTION

The ventral visual pathway is an integral part of the networks concerned with the processing of object quality [Kravitz et al., 2013]. For a substantial portion of this highly specialized part of the human visual system, retinotopic representations of the contralateral visual hemifield have been demonstrated [Arcaro et al., 2009; Brewer et al., 2005], similar those of other visual processing stages [Wandell et al., 2007]. Specifically, two adjacent visual field map clusters anterior to visual area 4 (V4) were identified that are involved in color, scene, and/or object processing [Arcaro, et al., 2009; Brewer, et al., 2005]. These reside in the ventral occipital (VO) and parahippocampal cortex (PHC). Each of these clusters comprises two retinotopic maps, i.e., the visual areas VO1 and VO2, and PHC1 and PHC2 [Arcaro et al., 2009]. In the present study we addressed, whether this organization scheme is imperative for these visual areas. For this purpose we investigated participants that had congenitally abnormal visual field representations in the early visual cortex because of misrouting of the optic nerves at the optic chiasm.

While the temporal and nasal retinae normally project to the ipsilateral and contralateral hemisphere, respectively, this projection scheme is altered in conditions with congenital malformations of the optic chiasm as seen in albinism and achiasma. In albinism, part of the projection of the temporal retina crosses the midline separating the two hemispheres and thus projects abnormally to the contralateral hemisphere [Apkarian, et al., 1983; Hoffmann, et al., 2005; von dem Hagen, et al., 2007]. In achiasma, the nasal retina fails to cross the midline and thus projects to the ipsilateral hemisphere [Apkarian, et al., 1994, 1995; Prakash et al., 2009]. In both conditions, the primary visual cortex (V1) receives substantial abnormal input from the ipsilateral visual field in addition to the normal input from the contralateral visual field. Specifically, a retinotopic map of the ipsilateral visual field is overlaid onto the normal map of the contralateral visual field [Davies-Thompson et al., 2013; Hoffmann et al., 2003, 2012; Muckli et al., 2009]. This organization of the primary visual cortex is likely to due to unaltered geniculo-striate connections, i.e., connections that follow the projection scheme also observed in participants with a normal optic chiasm [Guillery, 1986]. It is not known how this highly atypical monocular visual field representation in the early visual cortex is propagated to specialized higher tier processing stages in order to support visual pattern perception in albinism and achiasma [albinism: Wolynski et al., 2010; Klemen et al., 2012; achiasma: Victor et al., 2000]. Main elements of the relevant processing reside in the ventral visual cortex. Notably, the convolution of the ventral visual cortex is altered in albinism compared to controls [Bridge et al., 2012]. A potential cause of this altered cortical morphology might be the adaptation of the respective cortico-cortical connectivity in response to the abnormal representations of lower tier cortical input stages. For example, a rearrangement of the overlaid retinotopic maps of earlier visual areas could yield a contiguous retinotopic map that comprises both visual hemifields, an arrangement evident in some animal models of optic nerve misrouting [Guillery, 1986]. Such an adapted cortico-cortical connectivity would require a substantial scope of developmental plasticity in higher tier visual cortex. In contrast, the absence of rearranged maps would indicate unaltered cortico-cortical connectivity and thus an absence of such large scale plasticity of the underlying brain connectivity. Importantly, it is not imperative that the representation abnormalities are organized in the same way in lower and higher visual areas. In animal models of albinism different organization patterns were reported in striate and extrastriate cortex. Specifically, albinotic cats appear to display different visuotopic representations in striate and extrastriate cortex [Leventhal and Creel, 1985; Schmolesky et al., 2000] or even within striate cortex [Cooper and Blasdel, 1980].

To identify the scope of developmental plasticity that guides visual map formation in the human ventral processing stream, we examined fMRI-based retinotopic maps of the VO and the posterior PHC in participants with congenital misrouting of the optic nerves. To obtain generalizable conclusions, we included participants with two different types of optic chiasm malformations, i.e., with enhanced and with reduced crossing of the optic nerves, in an albinotic group and an achiasmic individual, respectively.

METHODS

Participants

Five controls [C1-5: normal decimal visual acuity ($\geq$1.0); aged 24–42 (median 27); 1 female], five participants with albinism [A1-5: aged 27–44 (median 37); 3 female; 4 with

oculo-cutaneous and one with ocular albinism (A3)] and one achiasmic participant (Ach1, aged 22, male) were examined. A1-5 had typical symptoms of albinism based on an ophthalmological examination (iris translucency and foveal hypoplasia) and albinotic visual evoked potential (VEP) lateralization indicative of misrouted optic nerves [Apkarian et al., 1983; Hoffmann et al., 2007a, 2011, von dem Hagen et al., 2008]. Ach1, previously described in detail [Hoffmann et al., 2012], was scanned at higher spatial resolution (2 mm isotropic voxels) for the present study. He had typical symptoms of achiasma (MRI confirmation of hypoplastic chiasma; see-saw nystagmus and achiasmic VEP lateralization [Apkarian et al., 1994]) and no indications of albinism. The decimal visual acuity of the tested eye was 0.15, 0.25, 0.5, 0.13, and 0.2, for A1-5, respectively, and 0.5 for Ach1 (refractive errors were corrected for the viewing distance in the MRI scanner with custom made frames or contact lenses). The horizontal nystagmus amplitude of the tested eye was 5.9°, 3.0°, <0.3°, 6.0°, and 6.0° for A1-5, respectively, and 3.5° for Ach1. No ophthalmological or neurological abnormalities apart form the ones detailed above were evident in the participants. All participants gave their informed written consent. The study was approved by the Ethics committee of the University of Magdeburg and followed the tenets of the Declaration of Helsinki.

Stimulus

All participants were stimulated monocularly, i.e., the left eye in controls and albinotic participants, the right eye in the achiasmic individual. As a consequence of this monocular stimulation scheme, the abnormal representation of the ipsilateral visual hemifield resides in all participants with misrouting on the right hemisphere. Conventional retinotopic hemifield mapping [Hoffmann et al., 2012] was performed. Two repetitions of polar angle mapping and of eccentricity mapping were obtained per hemifield, i.e., 8 scans (2 × 2 × 2 scans) in all participants, but A5 (only 5 out of 8 scans could be acquired, i.e. only condition rings in the right hemifield was repeated) and A3 (only 7 out of 8 scans were retained, as one scan (repetition of condition rings in the right hemifield) had to be discarded due to excessive head motion).

For retinotopic hemifield mapping [DeYoe et al., 1996; Engel et al., 1994, 1997; Sereno et al., 1995] at 7T magnetic field strength a section of a contrast reversing circular checkerboard stimulus (6 reversals/s, 90 cd/m^2 mean luminance) was presented in a rectangular mask (30° wide and 15° high). The stimulus contrast was set to 97% in the hemifield to be mapped and to 0% in the opposing hemifield, i.e., the leading edge of the wedge disappeared when moving into the opposing hemifield and reappeared again in the mapped hemifield later after 50% of the stimulus cycle. As a consequence, the phase range of the responses is expected to cover only 180° plus some phase jitter. Seven 36 s cycles of the stimulus were projected (DLA-G150CL, JVC Ltd.) on a screen using Presentation (NeuroBehavioral Systems). The stimulus stepped either as a rotating wedge through the polar angles for polar angle mapping (clockwise and counterclockwise for the left and right hemifield, respectively; wedge width: 90°) or as a contracting ring through the eccentricities for eccentricity mapping (ring was off-screen entirely for 7 s of the 36 s stimulus cycle before reappearing in the periphery; ring width: 0.82°). The participants were instructed to maintain fixation during stimulation and to report color changes of the central target (diameter: 0.25°) via button press. Fixation was monitored during the scans with an MR-compatible eye tracker [Kanowski et al., 2007].

Because of scanner availability participants A4 and A5 were scanned at 3T magnetic field strength. The same projector type as for the 7T scans was used, while the stimulus size exceeded that of the 7T stimulus (48° wide and 24° high; ring width: 1.3°; central target diameter: 0.4° diameter). The mean luminance was set to 25 cd/m^2 and the pattern contrast to 97%. In the analyses all relevant measures are related to participants' internal reference values to take into account differences of stimulus size and luminance for 7T and 3T scanning.

Data Acquisition

The MRI data were acquired at either 7T (Siemens Magnetom 7T) or 3T magnetic field strength (Siemens Verio). A previous comparative study demonstrated equivalent visual area borders for fMRI-based retinotopic mapping with both magnetic field strengths [Hoffmann et al., 2009]. At the 7T MRI system a 24-channel coil (CP transmit coil and 24 elements receive; Nova Medical, MA) was used. fMRI data were acquired using a multislice 2D gradient echo EPI sequence [Hoffmann et al., 2009] at either 2 mm (Ach1: TR: 2.4 s; TE: 22 ms; flip angle (FA): 80°; 44 axial slices; matrix size: 106 × 106; interleaved slice order without gap; field of view (FOV) 212 × 212 mm) or 2.5 mm isotropic resolution (C1-5, A1-3 TR: 2.4 s; TE: 21 ms, FA: 80°; 42 axial slices: matrix size: 80 × 80; interleaved slice order without gap; FOV: 200 × 200 mm). At the 3 T MRI system the lower part of a 32-channel-coil, comprising 20 elements, was used to guarantee an unobstructed view of the stimulus and fMRI data were acquired at 2.5 mm isotropic resolution (A4-5; TR 2.4 s; TE 30 ms; FA 80°; 38 axial 2.5 mm slices; matrix size: 80 × 80; interleaved slice order without gap; FOV 200 × 200 mm). Foam padding was used to minimize head motion. For each functional scan 110 volumes were acquired at a sampling interval of 2.4 s (duration: 4:24 [min:s], i.e., 7 1/3 stimulus cycles á 36 s). At 7T online distortion correction was applied [Zaitsev et al., 2004]. Further, T1 weighted, for 7 T inhomogeneity corrected [Van de Moortele et al., 2009], MPRAGE MR images were acquired at 1 mm isotropic resolution (7T: TR 2000 ms; TE 5.24 ms, TI 1050 ms; 3T: TR 2500 ms; TE 4.82 ms; TI 1100 ms) to

create a flattened representation of the cortical gray matter. Gray and white matter was segmented from the anatomical MRI scan using custom software [ITK Gray, 1.6.0.1. and MrGray (VISTA)] and hand-edited to minimize segmentation errors. Special care was taken to avoid cross talk between the gray matter of opposing hemispheres [Teo et al. 1997; Wandell et al., 2000].

Data Processing and Analysis

Preprocessing of the fMRI data comprised slice time correction and realignment to compensate for head motion [SPM5 (http://www.fil.ion.ucl.ac.uk/spm/) running with MATLAB 2009b]. Each voxel's time-series (TS) underwent the following analysis [MATLAB 2009b with Stanford VISTA-tools Repository 3435 (VISTA)]: (1) five temporal samples were discarded from the TS to avoid transient onset artefacts, (2) the TS were divided by the voxel's mean intensity, (3) the TS were filtered with a high-pass cut-off of 4 cycles/scan, (4) the TS of repeated experiments were averaged, (5) Fourier analysis was applied to the TS to obtain the amplitude and phase for each frequency, and (6) the coherence with a sinusoid with a frequency equal to that of the visual stimulation (1/36 Hz), was calculated [Engel et al., 1997]. After registration of the T1 weighted images to the T2* weighted images' coordinate frame the results of the coherence analysis were projected onto the flattened representation of the cortical surface (flatmap) [Engel et al., 1997]. Subsequently, the coherence and phase values were blurred by convolving a Gaussian kernel (1.7 mm full width at half maximum) with the complex vector representation. A coherence threshold of 0.26, i.e., corresponding to a significance threshold of $P < 0.005$, [Silver et al., 2005] was applied to retain the stimulus driven responses. Further, a phase window was applied to the polar angle mapping data, which exceeded the stimulation epoch of the stimulus cycle, i.e., 180°, by ±15%, i.e., 27°, to account for phase jitter. Dedicated functions available in VISTA-tools were used to determine the activated surface area. Further calculations were performed in IGOR Pro 6.22A (WaveMetrics, Lake Oswego, OR).

Delineation of Visual Areas

Diverging delineations and nomenclatures of the ventral human visual areas have been proposed in the past. These are likely due to inter-individual differences in the vasculature of this brain region [Winawer et al., 2010] and related to differences of the cortical organization in humans and macaque monkeys [Gattass et al., 1988]. We here adhere to the nomenclature reviewed in Wandell et al. [2007] and Silver and Kastner [2009]. According to this work, the previously described retinotopically organized areas of the ventral visual processing stream, i.e., V4, VO1, VO2, PHC1, and PHC2, comprise representations of the entire contralateral visual hemifield [Arcaro et al., 2009]. In the present study, these visual areas were delineated in each individual on the basis of the respective eccentricity and polar angle maps obtained with the above procedures following Brewer et al. [2005] and Arcaro et al. [2009]. Specifically, V4 is identified as a hemifield representation adjacent to the dorsal portion of ventral V3 (in contrast, in macaques V4 has a ventral and dorsal portion that comprise the upper and lower quadrant of the contralateral visual hemifield, respectively [Gattass et al., 1988]). The foveal representation of V4 resides at the occipital pole and is part of the eccentricity map also comprising V1, V2, and V3 [Wade et al., 2002]. V4's polar angle map is parallel to that of V3. The visual field clusters VO1/2 and PHC1/PHC2 are located anterior to V4. The polar angle maps and consequently the area borders of VO1, VO2, PHC1, and PHC2 are arranged perpendicular to the representation of the upper vertical meridian in V3, i.e., to the ventral border of ventral V3. The recognition of the representation of the upper vertical meridian in the polar angle maps allows for the identification of the VO1/VO2 and the PHC1/PHC2 border. The recognition of the representation of the lower vertical meridian allows for the identification of the VO2/PHC1 border. Further, while the more peripheral visual field representations reach the ventral V3 border, the central representations are located more ventrally. Thus the identification of the local minima of the eccentricity maps ventral to V3 allows for the confirmation of the location of the foveal confluence of the VO1/VO2 cluster and of the PHC1/PHC2 cluster.

Statistics

Two-way ANOVAs (factors: participant group and visual areas) were performed with SPSS 21 (IBM, NY) to assess (i) surface areas, (ii) phase maps, and (iii) response amplitudes. To reduce the degrees of freedom of the statistical models, we collapsed the visual areas into two groups of visual areas, early visual areas, i.e. covering V1, V2, and V3 and termed "V1/2/3", and higher areas of the ventral pathway, i.e., covering VO1, VO2, PHC1, and PHC2 and termed "VO/PHC". The similarity of the phase maps was assessed by correlating pairs of the obtained phase maps with each other using circular statistics implemented in MATLAB [Berens, 2009] to take the circular nature of the phase data into account. The resulting correlation coefficients were z-transformed prior to statistics. The sphericity assumption was met for phase maps and response amplitudes.

RESULTS

Cortical Representations of Polar Angles and Eccentricities

For a qualitative assessment of the polar angle and eccentricity mapping data, we projected the phase values of suprathreshold voxels onto the flattened representation of the right

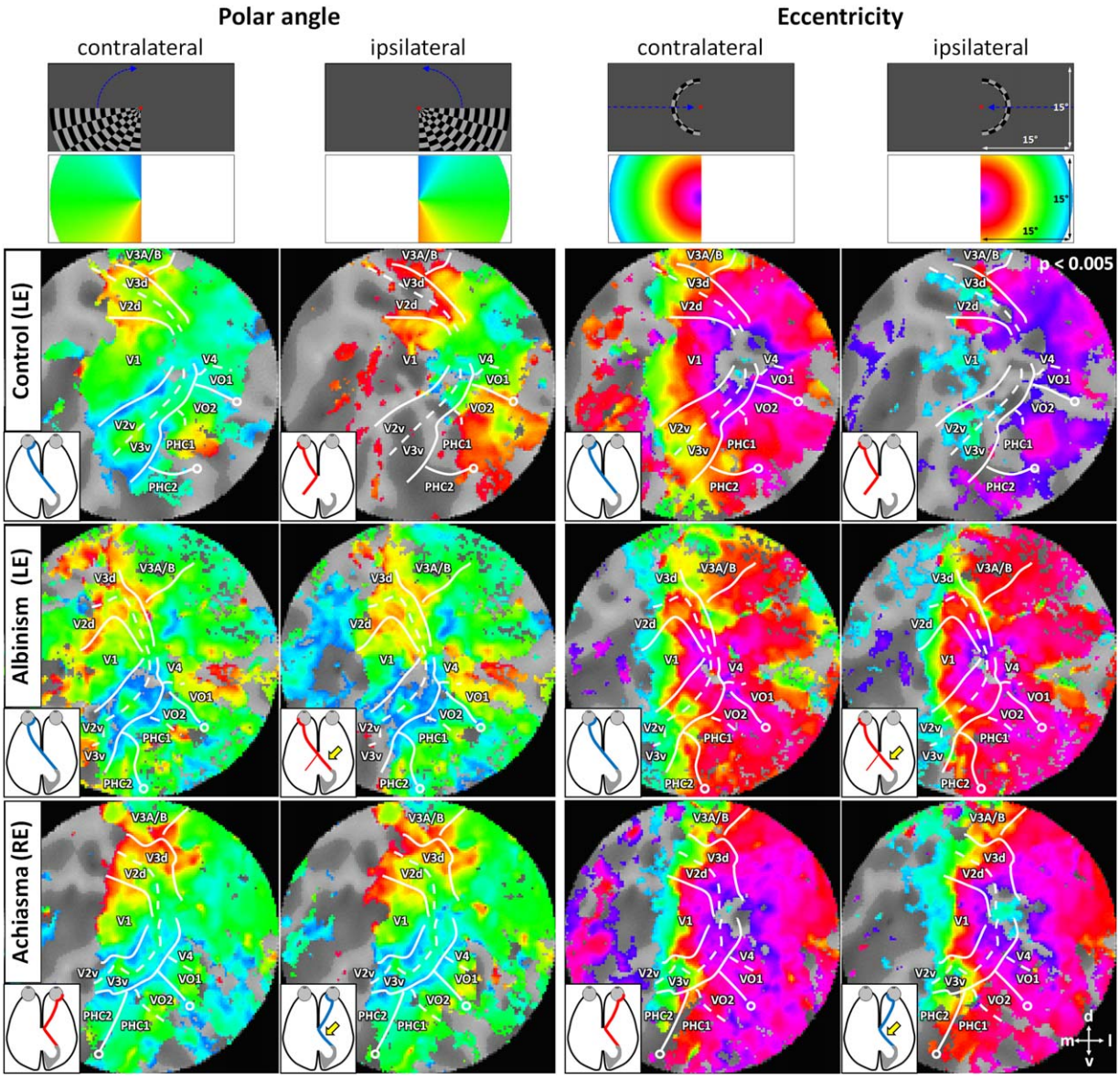

Figure 1.

Flattened representations of the right occipital lobe for representative individuals of the investigated cases, i.e., control (C1; left eye stimulated), albinism (A1; left eye stimulated), and achiasma (Ach1; right eye stimulated). The superthreshold phase maps for polar angle and eccentricity mapping in the contra- and ipsilateral visual hemifield are projected onto the flatmaps. For all individuals orderly mappings of the contralateral visual hemifield were evident, which allowed for the identification of early and ventral visual areas. In the control, ipsilateral mappings were restricted partly to representations of the vertical meridian and the central visual field and to spurious activations presumably due to negative BOLD modulations. In albinism and achiasma, extensive orderly mappings of the ipsilateral visual hemifield were evident that resembled those of the contralateral hemifield. The inferred optic nerve projection is given in the insets, abnormal projections are indicated with a yellow arrow. The top row indicates stimulus schematics; second row depicts color codes (see Methods for details). Open circles indicate a representation of the visual field center; lines indicate visual area boundaries (representation of horizontal and vertical meridians) as inferred from the polar angle maps to stimulation in the contralateral visual hemifield. Abbreviations: V1–4: visual areas 1–4; PHC 1/2: parahippocampal cortex 1/2; VO 1/2: ventral occipital areas 1/2.

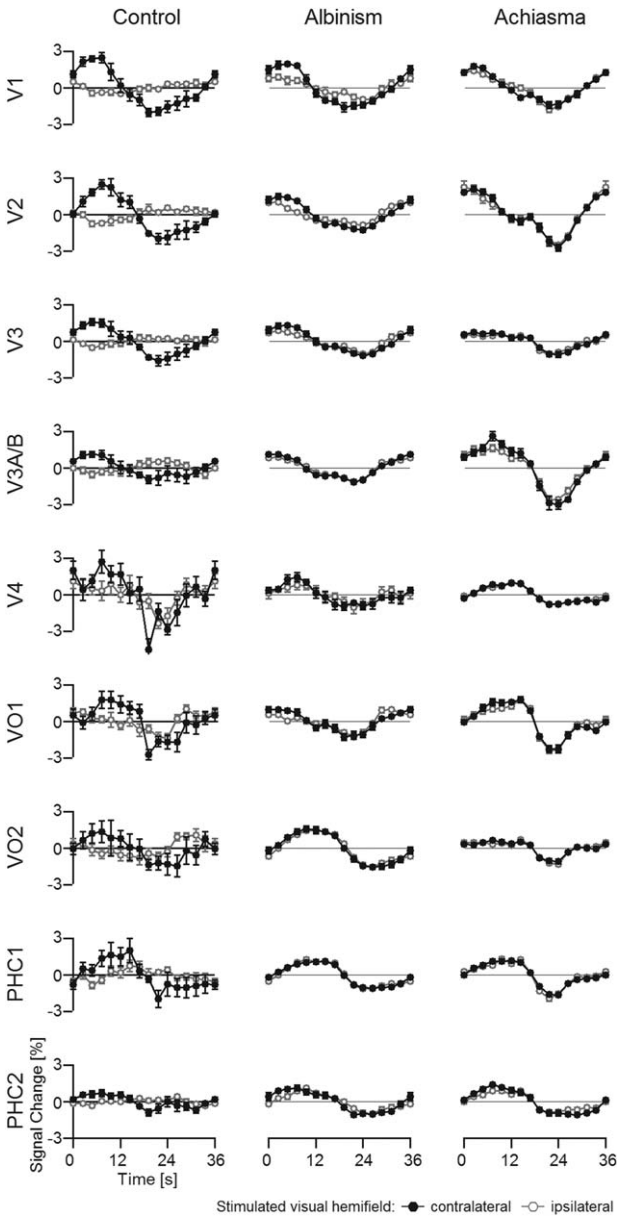

Figure 2.

Times series of the polar angle mapping data presented in Figure 1 (average across all voxels of the respective visual area; average across 7 cycles ± SEM). Positive BOLD responses are expected predominantly during the first half of the stimulation cycle (as detailed in Methods section). It should be noted that apparent area-related phase shifts within this hemicycle are a natural consequence of different contributions of specific polar angles to the respective average responses. The ROIs comprised voxels that were significantly driven for stimulation in the contralateral visual hemifield. Importantly, even in the areas PHC1/2, stimulation in either hemifield evoked comparable responses in albinism and achiasma, but not in the control, where positive BOLD responses were obtained for contralateral hemifield stimulation only. For expansion of the area labels see Figure 1.

occipital lobe (Fig. 1 for a representative example of controls, albinism, and achiasma). For all conditions, i.e. controls, albinism, and achiasma, extensive significant BOLD-responses were evident in the visual cortex for stimulation in the contralateral visual hemifield. The responses covered the early visual cortex and large parts of the ventral visual cortex. The respective phase signatures were in accordance with those previously described [Wandell et al., 2007], which allowed for the delineation of the early visual areas and of the ventral visual areas V4, VO1, VO2, PHC1, and PHC2. These areas have previously been described to comprise representations of the contralateral hemifield with characteristic eccentricity and polar angle maps [Arcaro et al., 2009; Brewer et al., 2005]. While V4 is part of the eccentricity map that also comprises the early extrastriate cortex with a foveal representation at the occipital pole, the eccentricity maps of VO1/2 and PHC1/2 border ventral V3. Their peripheral visual field representations reach the ventral V3 border, the central representations are located more ventrally. As detailed in Methods, VO1/2 and PHC1/2 can generally be delineated from each other along the representations of the vertical meridian from polar angle maps, and the foveal confluence of the VO1/VO2 and of the PHC1/PHC2 cluster can be confirmed from eccentricity maps. Within the limits of their interindividual variability [Arcaro et al., 2009; Brewer et al., 2005], the above characteristics of the phase signatures of the ventral areas were evident in the participants of the present study. In contrast to the areas of the ventral stream, the areas dorsal to the early visual areas, could, apart from V3A/B, not be delineated reliably in most of the participants and were therefore not assessed in the present study. In contrast to the passive viewing hemifield mapping applied in the present study, task engaging mapping might be required to obtain sufficient hemifield maps of the intraparietal sulcus [e.g., Konen and Kastner, 2008].

For stimulation in the ipsilateral visual hemifield, we obtained sparse responses for the controls. These were, in accordance with previous reports [Hoffmann et al., 2003; Tootell et al., 1998], mostly confined to the representations of the central visual field and of the vertical meridian, and to some intrusions of negative BOLD responses [Shmuel et al., 2006; Smith et al., 2000, 2004]. For albinism and achiasma, however, we observed extensive responses to stimulation in the ipsilateral visual hemifield in great expanses of the visual cortex. This is not only evident from the phase maps depicted in Figure 1, but also from the average time courses of the BOLD-responses during polar angle mapping depicted in Figure 2. While in albinism and achiasma the time courses were similar for stimulation in opposing hemifields, they differed for the controls, i.e., sizable BOLD responses were only evident for stimulation in the contralateral visual hemifield.

In albinism and achiasma, responses to ipsilateral stimulation resulted in systematic phase maps of the ipsilateral

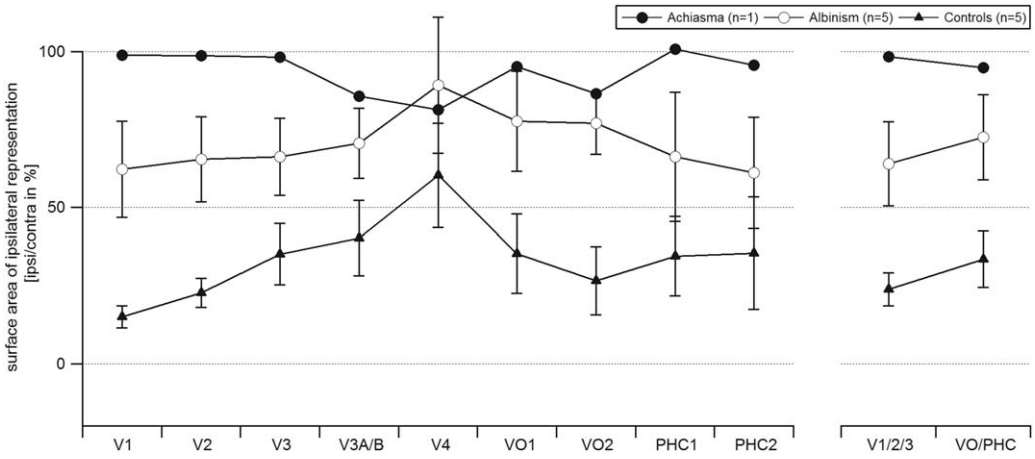

Figure 3.

Relative surface area of the ipsilateral representation. The respective correlation coefficients are given as a function of visual area for controls, albinism, and achiasma (mean ± SEM). Statistics were computed for the visual area groups V1/2/3 and VO/PHC as detailed in Methods section. The control group and the albinotic group differ significantly, but independent of visual area group as detailed in Results. For expansion of the area labels see Figure 1.

hemifield. This applied to both the responses of early visual cortex and for areas of the ventral processing stream, i.e., VO1, VO2, PHC1, and PHC2. Remarkably, these maps were to a large extent similar to those of the contralateral visual hemifield. This indicates a systematic mirror-symmetrical overlay of retinotopic maps not only in early visual areas, but also in the ventral processing stream of the visual cortex contra- and ipsilateral to the stimulated eye in albinism and achiasma, respectively. These findings are likely due to a propagation of the organization pattern of the early visual cortex, i.e., an overlaid retinotopic representation of opposing hemifields, to the ventral visual processing stream. We detailed the characteristics of the obtained maps systematically in three separate quantitative analyses that compared the responses to stimulation in the ipsi- and contralateral hemifield with respect to activated cortical surface area, phase maps, and response amplitudes.

Extent of the Representation of the Ipsilateral Visual Field

To quantify the relative extent of the representation of the ipsilateral visual field we determined the activated cortical surface area, i.e., comprising voxels that exceed a significance threshold of $p < 0.005$, for stimulation in the ipsi- and contralateral hemifield. Subsequently we calculated the relative activated ipsilateral surface area (surface area$_{\text{ipsilateral stimulation}}$/surface area$_{\text{contralateral stimulation}}$ × 100%) for each visual area (i.e., V1, V2, V3, V3A/B, V4, VO1/2, PHC1/2) as depicted in Figure 3. For these areas taken together the relative activated ipsilateral surface area was 27 ± 5%, 66 ± 13%, and 96% in the control group, the albinism group, and in the achiasmic individual, respectively. This supports previous reports that the representation abnormality in albinism is associated with partial optic nerve misrouting of varying degree [Creel et al., 1981; Hoffmann et al., 2003, 2005;von dem Hagen et al., 2007], while it is associated with more complete misrouting in achiasma [Hoffmann et al., 2012; Prakash et al., 2009] as evident from Figure 1. In fact, an analysis of the phase maps of V1 obtained from the five participants with albinism demonstrated that the abnormal representation of the ipsilateral horizontal meridian varied within a range of 3.6° to 13.0° [horizontal extent in A1 to A5: 12.7°, 3.6°, 10.2°, 13.0°, 5.9°]. To assess the significance of the representation abnormality and its dependence on visual area, we compared the control and the albinism group data, i.e. the relative activated ipsilateral surface area, in a two-way-ANOVA [factors: participant group (controls and albinism) and visual areas (V1/2/3 and VO/PHC)]. This analysis confirmed the group difference ($F(1,16) = 13.12$, $P = 0.002$), while neither the factor visual area ($F(1,16) = 0.679$, $P = 0.422$) nor the interaction of the factors group × visual area were significant ($F(1,16) = 0.002$, $P = 0.961$). This finding indicated a largely undiminished propagation of the abnormal representation in the early visual areas to advanced processing stages in the ventral visual cortex in albinism.

Cortical Overlay of the Representations of Opposing Hemifields

To determine the organization of the additional input to the visual cortex we conducted a detailed comparison of the phase maps for ipsi- and contralateral stimulation. From Figure 1 similar phase maps are evident for

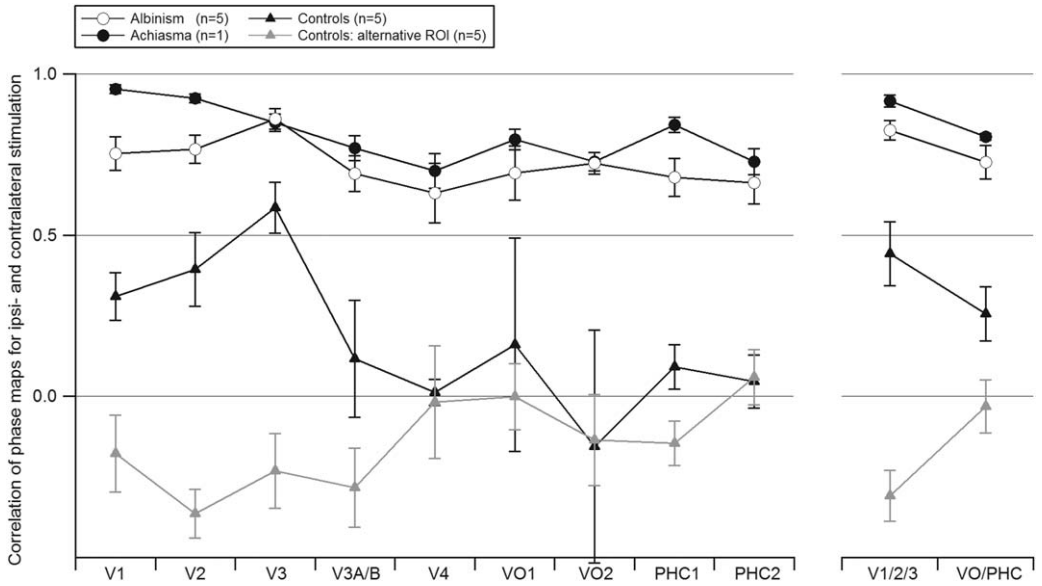

Figure 4.

Comparison of the phase maps of the right occipital lobe obtained for stimulation in the ipsi- and the contralateral hemifield. The respective correlation coefficients are given as a function of visual area for controls, albinism, and achiasma (mean ± SEM). Statistics were computed for the visual area groups V1/2/3 and VO/PHC as detailed in Methods. The control group and the albinotic group differ significantly, but independent of the visual area group. In addition to the data from ROIs, defined by voxels driven by stimulation in the ipsilateral visual hemifield, data from an "alternative ROI", defined by voxels driven by stimulation in the contralateral visual hemifield are presented for the control group. For expansion of the area labels see Figure 1.

stimulation in opposing hemifields in albinism and achiasma. These maps indicate that the cortical representations of opposing visual hemifields are organized as retinotopic cortical overlays of mirror-symmetrical positions in the visual field, not only in early but also in higher visual areas. To assess this in a quantitative manner, we applied correlation analyses to determine the similarity of the phase maps obtained for opposing hemifields (Fig. 4). We conducted these analyses for ROIs that were restricted to supra-threshold voxels ($P < 0.005$) upon stimulation of the ipsilateral visual field (ROI_{ipsi}) and to the phase window of the stimulation epoch for polar angle and eccentricity mapping (see Methods section). This way we ensured, in particular for albinism with its interindividually variable extent of the abnormal representation [Hoffmann et al., 2005], that only voxels were included that were driven by ipsilateral stimulation. For the control group this selection yielded ROIs that were confined to the residual representation of the ipsilateral hemifield. As a reference we included an additional depiction of the control data using ROI definitions that were based on voxels driven by contralateral stimulation ("alternative ROI" in Fig. 4). Comparing phase maps for ipsi- and contralateral stimulation with the correlation analysis, we obtained for all visual areas assessed, higher correlation values for albinism and achiasma than for controls. This indicated that in albinism and achiasma cortical representations of opposing visual hemifields were organized in similar retinotopic maps. Correspondingly, a two-way ANOVA [factors: participant group (controls and albinism) and visual areas (V1/2/3 and VO/PHC)] for ROI_{ipsi} demonstrated a significant difference between the correlation coefficients of the albinism and the control group ($F(1,16) = 35.299$, $P < 0.001$), while there was no significant effect for visual areas ($F(1,16) = 3.761$, $P = 0.07$). Importantly, there was no significant interaction of participant group × visual area ($F(1,16) = 0.203$, $P = 0.658$). This underlines that the organization of visual input from opposing hemifields as a retinotopic overlay is preserved in the ventral processing stream.

Relative Strength of the Cortical Responses to Stimulation of Opposing Hemifields

With the above analyses we demonstrated for albinism and achiasma that the same voxels that were driven by the ipsilateral visual field, i.e., ROI_{ipsi}, were also driven by the contralateral visual field, i.e., by a mirror symmetrical visual field location with respect to the vertical meridian. In a further analysis we determined, whether these voxels responded with the same strength to both hemifields. In Figure 5 the response amplitudes of the ipsilateral

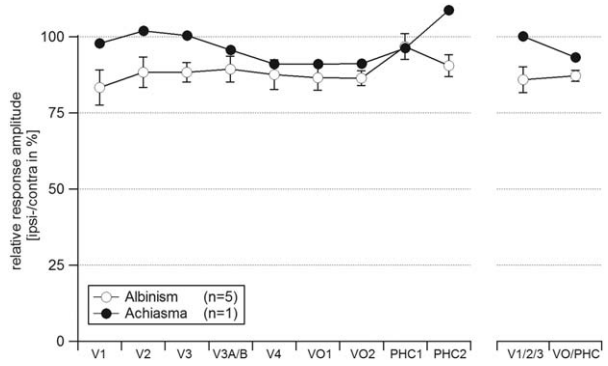

Figure 5.

Relative response amplitudes to stimulation in the ipsilateral visual hemifield. The amplitudes are given as a function of visual area for albinism (mean ± SEM) and achiasma. For expansion of the area labels see Figure 1.

representation are given as the percentage of the response amplitude of the contralateral representation, i.e., the relative response. For the albinotic group we observed a small, but significant reduction of the responses of the representation of the ipsilateral hemifield (average relative response ± SEM: 86 ± 4%). A two-way-ANOVA, comparing the response amplitudes obtained for stimulation in the contra- and ipsilateral visual field across visual areas (factors hemifield stimulated [contralateral and ipsilateral ($F(1,68) = 6.942$, $P = 0.01$] and visual areas [V1/2/3 and VO/PHC; $F(1,68) = 1.13$, $P = 0.292$]), demonstrated that this hemifield-specific reduction was independent of the visual areas stimulated (nonsignificant interaction of factors hemifield stimulated and visual areas, $F(1,68) = 0.204$, $P = 0.653$). No such response reduction was observed in the achiasmic individual [average relative response: 99%]. We assume that the slight amplitude reduction for albinism might be due to the fact that it is only a part of the ipsilateral hemifield that is abnormally represented in albinism and that some voxels that were included in ROI_{ipsi} reflect the transition zone with naturally less ipsilateral responses. In that case it would be expected that the exclusion of this transition zone from the ROIs ($ROIs_{restricted}$) might yield, as compared to the original ROIs ($ROIs_{original}$), higher amplitude measures. We tested this specifically in three participants with albinism and sufficiently big ROIs of the abnormal representation in all visual areas of interest (V1/2/3, VO1/2, and PHC1/2). For this purpose, we created $ROIs_{restricted}$ that were centered with respect to $ROIs_{original}$ and shrunk to ~25% of the $ROIs_{original}$ area. As a consequence, these ROIs were focused on the cortical representations of the horizontal meridian that are dominated by the overlay of abnormal and normal representation. We observed a slight but nonsignificant trend of increased amplitudes for $ROIs_{restricted}$ (V1/2/3, $ROIs_{original}$ vs. $ROIs_{restricted}$: 83.6% ± 2.7% vs. 88.4% ± 6.1%; VO/PHC, $ROIs_{original}$ vs. $ROIs_{restricted}$: 91.8% ± 9.9% vs. 93.8 ± 3.9).

DISCUSSION

We report abnormal visual field maps in the ventral visual cortex of individuals with congenitally abnormal input to the primary visual cortex that is caused by enhanced or reduced crossing of the optic nerves at the chiasm in albinism and achiasma, respectively. The retinotopic representations of opposing hemifields were superimposed in the visual field map clusters VO1/2 and PHC1/2, an arrangement also evident in the early visual cortex of these individuals. Consequently, an exclusive retinotopic organization of the contralateral visual hemifield is not imperative for the organization of visual areas of the ventral pathway. Instead, it appears that the visual field map clusters VO1/2 and PHC1/2 follow the gross-organization scheme that is evident in lower tier visual cortex even if this is abnormal. A potential mechanism underlying this organization pattern would be the unaltered propagation of the organization in the earlier visual cortex to downstream areas via largely unaltered cortico-cortical connections despite abnormal input to V1.

Plausibility of the Observed Cortical Mapping

The mappings we report for the early visual cortex of individuals with congenital malformations of the optic chiasm are in close agreement to earlier reports of independent measurements in different (albinism [Hoffmann et al., 2003]; achiasma [Davies-Thompson et al., 2013; Hoffmann et al., 2012, participant AC2]), or the same participants (achiasma [Hoffmann et al., 2012, participant AC1]) and confirm the previously reported cortical overlay of retinotopic maps of opposing visual hemifields in early visual cortex. The results are also in agreement, though partial, with those previously reported in an extremely unusual case, i.e., an individual who lost one hemisphere during embryonic development [Muckli et al., 2009]. Even here overlaid representations were evident in the dorsal portions of V1 and V2. In ventral V2, however, islands of nonoverlapping maps were observed, which might be related to alterations in the underlying reorganization or/and to the effect of circumscribed defects in the upper visual hemifield field of that individual.

Some participants of the present and of previous studies have sizable nystagmus. While small-amplitude nystagmus and other fixation instabilities have little impact on the characterization of retinotopic maps [Baseler et al., 2011; Levin et al., 2010], an impact of larger amplitudes cannot be excluded per se. As similar early visual cortex mappings were previously reported for individuals with albinism with horizontal nystagmus amplitude below and above 2 deg such effects appear to be negligible [Hoffmann et al., 2003], but the potential effects of nystagmus still deserve evaluation. Fixation instabilities centered around fixation could introduce spatial blur, which spreads the signal across the cortex and reduces the signal-to-noise-ratios of the signals, but would not cause sizable spurious retinotopic maps. They would thus leave

the conclusions of the present and previous studies largely unaffected. In contrast, a systematic deviation from central fixation might have a stronger effect on the retinotopic mapping signatures. It would have a distinct effect particularly on the eccentricity maps of the central visual field, i.e., inverted phase progressions along the representation of the horizontal meridian. While such effects would be strongest in areas with extended representations of the visual field centre, i.e., V4 and VO1/2 [Arcaro et al., 2009], they should already be evident at the input stage of the visual cortex, i.e., V1, where they can be judged best due to the size of this area and the clarity of the phase signatures [Winawer et al., 2010]. Such phase inversions were not observed (Fig. 1).

Visual Function in the Presence of Large-Scale Cortical Representation Abnormalities

In the presence of enhanced or reduced crossing of the optic nerves at the chiasm the organization of the visual field maps in all visual areas examined follows a largely similar pattern, namely that of overlaid retinotopic representations of opposing hemifields. Still visual function is relatively unaffected, with the exception of nystagmus and the absence of stereopsis. The affected individuals make effective use of their vision in daily life, including sport activities and reading [Apkarian et al., 1994, 1995; Hoffmann et al., 2012; Prakash et al., 2009; Victor et al., 2000]. Visual field sensitivities are largely normal. In particular, there are no visual field defects that are specifically associated with the abnormal representation of the nasal retina [Hoffmann et al., 2007b, 2012]. Further, there is no evidence for perceptual crosstalk across opposing visual hemifields, neither in achiasma [Victor et al., 2000] nor in albinism [Klemen et al., 2012], as it might be expected from the cortical overlay of opposing hemifields. Finally, pattern and object perception and object recognition do not appear to be selectively impaired [Klemen et al., 2012; Victor et al., 2000; Wolynski et al., 2010]. While, lesions in the ventral visual cortex severely impair object recognition [Konen et al., 2011], it appears that a pronounced mapping abnormality in these areas is not necessarily associated with a distinct dysfunctionality. This suggests that normal mapping is not imperative for the general functionality of the ventral visual cortex. Future specific psychophysical examinations to detail the integrity of visual object perception will help to identify the limits of the preservation of normal function in the presence of the abnormal mappings described in the present study.

Early Visual Cortex Organization in Congenital Chiasmatic Malformations

The consequences of chiasmatic abnormalities on the organization of the visual cortex have been studied in detail in various models of albinism in order to uncover how the additional input from the ipsilateral visual hemifield is represented at the level of the visual cortex. Remarkably, three different cortical organization patterns were found in non-primates [reviewed in Guillery, 1986]. The geniculo-striate connections can be (a) reordered to yield a contingent retinotopic representation of both visual hemifields ("Boston pattern"), (b) unaltered, but not driving activity in the visual cortex due to intracortical suppression ("Midwestern pattern"), (c) unaltered and driving the macroscopically superimposed cortical representations of opposing hemifields ("true albino pattern"). Importantly, the latter pattern is the only one so far reported in primates [Davies-Thompson, et al., 2013; albinism: Guillery et al., 1984; achiasma: Hoffmann et al., 2003, 2012] and was also confirmed in the present study. The true albino pattern is likely due to a reassignment of the cortical ocular dominance columns to hemifield dominance columns [Guillery, 1986]. This reassignment is the direct consequence of unaltered geniculo-striate projections, which normally result in interleaved cortical representations of the two eyes, i.e., ocular dominance columns. In the case of misrouted optic nerves, however, they result in interleaved cortical representations of monocular input from opposing visual hemifields, i.e., hemifield dominance columns. A cortical organization that follows the "true albino pattern" at the stage of the primary visual cortex is therefore a simple way to allocate resources for the additional representation of the ipsilateral visual field, since it is based on reassigning the resources normally used for processing the, now missing, input from the ipsilateral eye in albinism and the contralateral eye in achiasma.

Higher Visual Cortex Organization in Congenital Chiasmatic Malformations

We report evidence for macroscopically superimposed retinotopic maps of opposing visual hemifields not only in the primary and early visual cortex, but also in higher processing stages. A likely mechanism for the propagation of this organization pattern through the visual cortex, are largely unaltered cortico-cortical projections. This way the organization pattern of early visual areas would be adopted by higher visual areas. Such a conservative mechanism appears to prevail even for the specialized visual field maps in the PHC.

Incorporating a representation of the ipsilateral visual field is much more demanding at the level of extrastriate and higher tier visual cortex, since at this stage many neurons normally receive predominantly binocular input [Felleman and Van Essen, 1987; Maunsell and Van Essen, 1983; Tanabe et al., 2005]. Consequently there are, in contrast to V1, no spare resources in albinism and achiasma that would normally be selectively concerned with processing the monocular input that is missing in albinism or achiasma. As a consequence, part

of the neural resources normally available for processing the contralateral visual field must be made available for processing the additional input from the ipsilateral visual field. Remarkably, the relative responses of the ipsilateral representation [$\text{amplitude}_{\text{ipsilateral representation}}/\text{amplitude}_{\text{contralateral representation}} \times 100$ (%) as depicted in Fig. 4] did not differ between striate, extrastriate cortex, and the two visual field map clusters in the ventral processing stream, i.e., the VO cortex and the posterior PHC, neither in albinism and nor in achiasma. This demonstrated undiminished processing of the additional visual input up to higher levels of visual processing. We conclude that the mechanisms that govern the allocation of neural resources for processing of the additional visual input appear to be operating with a similar effectiveness for striate, extrastriate, and higher tier visual areas.

Finally, the remote representation of corresponding parts of the visual field, i.e., on opposing hemispheres, in albinism and achiasma might induce changes to the interhemispherical information flow via the splenial callosal connections. Diffusion tensor imaging studies revealed largely unaltered interhemispheric splenial connections in achiasma [Hoffmann et al., 2012; Davies-Thompson et al., 2013], but the issue deserves to be studied in more detail and to be extended to albinism.

Principles of Visual System Organization in Achiasma and Albinism

From the direct juxtaposition of the organization of the visual cortex in albinism and achiasma general principles governing map formation in the human visual cortex can be inferred. In both types of visual pathway abnormalities, i.e. enhanced and reduced optic nerve crossing, visual hemifields are made available for visual perception [Hoffmann et al., 2007b, 2012; Klemen et al., 2012; Victor et al., 2000; Wolynski et al., 2010]. As detailed above, a combination of unaltered development of the thalamocortical and cortico-cortical connections on the one hand, and an adaptation of intracortical connections, e.g., experience driven cortical pruning [Sinha and Meng, 2012], on the other hand, might serve to mediate an independent visual perception in opposing visual hemifields in both human albinism and human achiasma [Hoffmann et al., 2012; Klemen et al., 2012]. In contrast, a variety of mechanisms appear to be available in nonprimate animal models of albinism, even within the same species or individual [reviewed in: Guillery, 1986; Hoffmann et al., 2003]. One of these, the Midwestern pattern, actually fails to translate the additional visual input into visual perception, which results in selective visual field defects [Elekessy et al., 1973; Garipis and Hoffmann, 2003] that are not evident in primates with chiasmal abnormalities [Guillery et al., 1984; Hoffmann et al., 2007b; Muckli et al., 2009]. In contrast, uniform developmental mechanisms that reflect an interplay of plasticity and stability govern the development of the primate visual system and preserve fundamental aspects of visual function despite abnormal visual field representations even for high-level visual processing.

ACKNOWLEDGMENT

The authors are particularly grateful for the cooperation of the participants.

REFERENCES

Apkarian P, Reits D, Spekreijse H, van Dorp D (1983): A decisive electrophysiological test for human albinism. Electroenceph Clin Neurophysiol 55:513–531.

Apkarian P, Bour L, Barth PG (1994): A unique achiasmatic anomaly detected in non-albinos with misrouted retinal-fugal projections. Eur J Neurosci 6:501–507.

Apkarian P, Bour LJ, Barth PG, Wenniger-Prick L, Verbeeten B Jr (1995): Non-decussating retinal-fugal fibre syndrome. An inborn achiasmatic malformation associated with visuotopic misrouting, visual evoked potential ipsilateral asymmetry and nystagmus. Brain 118 (Pt 5):1195–1216.

Arcaro MJ, McMains SA, Singer BD, Kastner S (2009): Retinotopic organization of human ventral visual cortex. J Neurosci 29:10638–10652.

Baseler HA, Gouws A, Haak KV, Racey C, Crossland MD, Tufail A, Rubin GS, Cornelissen FW, Morland AB (2011): Large-scale remapping of visual cortex is absent in adult humans with macular degeneration. Nature Neurosci 14:649–655.

Berens P (2009): CircStat: A MATLAB toolbox for circular statistics. J Stat Software 31:1–21.

Brewer AA, Liu J, Wade AR, Wandell BA (2005): Visual field maps and stimulus selectivity in human ventral occipital cortex. Nat Neurosci 8:1102–1109.

Bridge H, von dem Hagen EA, Davies G, Chambers C, Gouws A, Hoffmann M, Morland AB (2012): Changes in brain morphology in albinism reflect reduced visual acuity. Cortex. [Epub ahead of print].

Cooper ML, Blasdel GG (1980): Regional variation in the representation of the visual field in the visual cortex of the Siamese cat. J Comp Neurol 193:237–253.

Creel D, Spekreijse H, Reits D (1981): Evoked potentials in albinos: Efficacy of pattern stimuli in detecting misrouted optic fibers. Electroencephalogr Clin Neurophysiol 52:595–603.

Davies-Thompson J, Scheel M, Jane Lanyon L, Sinclair Barton JJ (2013): Functional organisation of visual pathways in a patient with no optic chiasm. Neuropsychologia 51:1260–1272.

DeYoe EA, Carman GJ, Bandettini P, Glickman S, Wieser J, Cox R, Miller D, Neitz J (1996): Mapping striate and extrastriate visual areas in human cerebral cortex. Proc Natl Acad Sci U S Am 93:2382–2386.

Elekessy EI, Campion JE, Henry GH (1973): Differences between the visual fields of Siamese and common cats. Vis Res 13:2533–2543.

Engel SA, Rumelhart DE, Wandell BA, Lee AT, Glover GH, Chichilnisky EJ, Shadlen MN (1994): fMRI of human visual cortex. Nature 369:525.

Engel SA, Glover GH, Wandell BA (1997): Retinotopic organization in human visual cortex and the spatial precision of functional MRI. Cereb Cortex 7:181–192.

Felleman DJ, Van Essen DC (1987): Receptive field properties of neurons in area V3 of macaque monkey extrastriate cortex. J Neurophysiol 57:889–920.

Garipis N, Hoffmann KP (2003): Visual field defects in albino ferrets (Mustela putorius furo). Vis Res 43:793–800.

Gattass R, Sousa AP, Gross CG (1988): Visuotopic organization and extent of V3 and V4 of the macaque. J Neurosci 8:1831–1845.

Guillery RW (1986): Neural abnormalities in albinos. Trends Neurosci 18:364–367.

Guillery RW, Hickey TL, Kaas JH, Felleman DJ, Debruyn EJ, Sparks DL (1984): Abnormal central visual pathways in the brain of an albino green monkey (Cercopithecus aethiops). J Comp Neurol 226:165–183.

Hoffmann MB, Tolhurst DJ, Moore AT, Morland AB (2003): Organization of the visual cortex in human albinism. J Neurosci 23: 8921–8930.

Hoffmann MB, Lorenz B, Morland AB, Schmidtborn LC (2005): Misrouting of the optic nerves in albinism: Estimation of the extent with visual evoked potentials. Invest Ophthalmol Vis Sci 46:3892–3898.

Hoffmann MB, Schmidtborn LC, Morland AB (2007a): [Abnormal representations in the visual cortex of patients with albinism: Diagnostic aid and model for the investigation of the self-organisation of the visual cortex]. Ophthalmologe 104:666–673.

Hoffmann MB, Seufert PS, Schmidtborn LC (2007b): Perceptual relevance of abnormal visual field representations—Static visual field perimetry in human albinism. Br J Ophthalmol 91:509–513.

Hoffmann MB, Stadler J, Kanowski M, Speck O (2009): Retinotopic mapping of the human visual cortex at a magnetic field strength of 7T. Clin Neurophysiol 120:108–116.

Hoffmann MB, Wolynski B, Bach M, Meltendorf S, Behrens-Baumann W, Golla F (2011): Optic nerve projections in patients with primary ciliary dyskinesia. Invest Ophthalmol Vis Sci 52: 4617–4625.

Hoffmann MB, Kaule FR, Levin N, Masuda Y, Kumar A, Gottlob I, Horiguchi H, Dougherty RF, Stadler J, Wolynski B, Speck O, Kanowski M, Liao YJ, Wandell BA, Dumoulin SO (2012): Plasticity and stability of the visual system in human achiasma. Neuron 75:393–401.

Kanowski M, Rieger JW, Noesselt T, Tempelmann C, Hinrichs H (2007): Endoscopic eye tracking system for fMRI. J Neurosci Methods 160:10–15.

Klemen J, Hoffmann MB, Chambers CD (2012): Cortical plasticity in the face of congenitally altered input into V1. Cortex 48: 1362–1365.

Konen CS, Kastner S (2008): Representation of eye movements and stimulus motion in topographically organized areas of human posterior parietal cortex. J Neurosci 28:8361–8375.

Konen CS, Behrmann M, Nishimura M, Kastner S (2011): The functional neuroanatomy of object agnosia: A case study. Neuron 71:49–60.

Kravitz DJ, Saleem KS, Baker CI, Ungerleider LG, Mishkin M (2013): The ventral visual pathway: an expanded neural framework for the processing of object quality. Trends Cogn Sci 17:26–49.

Leventhal AG, Creel DJ (1985): Retinal projections and functional architecture of cortical areas 17 and 18 in the tyrosinase-negative albino cat. J Neurosci 5:795–807.

Levin N, Dumoulin SO, Winawer J, Dougherty RF, Wandell BA (2010): Cortical maps and white matter tracts following long period of visual deprivation and retinal image restoration. Neuron 65:21–31.

Maunsell JH, Van Essen DC (1983): Functional properties of neurons in middle temporal visual area of the macaque monkey. II. Binocular interactions and sensitivity to binocular disparity. J Neurophysiol 49:1148–1167.

Muckli L, Naumer MJ, Singer W (2009): Bilateral visual field maps in a patient with only one hemisphere. Proc Natl Acad Sci U S Am 106:13034–13039.

Prakash S, Dumoulin SO, Fischbein N, Wandell BA, Liao YJ (2009): Congenital achiasma and see-saw nystagmus in VACTERL syndrome. J Neuroophthalmol 30:45–48.

Schmolesky MT, Wang Y, Creel DJ, Leventhal AG (2000): Abnormal retinotopic organization of the dorsal lateral geniculate nucleus of the tyrosinase-negative albino cat. J Comp Neurol 427:209–219.

Sereno MI, Dale AM, Reppas JB, Kwong KK, Belliveau JW, Brady TJ, Rosen BR, Tootell RB (1995): Borders of multiple visual areas in humans revealed by functional magnetic resonance imaging.[see comment]. Comment in: Science. 1995; 268:803–804; PMID: 7754365. Science (New York, N.Y, 268: 889–893.

Shmuel A, Augath M, Oeltermann A, Logothetis NK (2006): Negative functional MRI response correlates with decreases in neuronal activity in monkey visual area V1. Nat Neurosci 9:569–577.

Silver MA, Kastner S (2009): Topographic maps in human frontal and parietal cortex. Trends Cogn Sci 13:488–495.

Silver MA, Ress D, Heeger DJ (2005): Topographic maps of visual spatial attention in human parietal cortex. J Neurophysiol 94: 1358–1371.

Sinha P, Meng M (2012): Superimposed hemifields in primary visual cortex of achiasmic individuals. Neuron 75:353–355.

Smith AT, Singh KD, Greenlee MW (2000): Attentional suppression of activity in the human visual cortex. Neuroreport 11: 271–277.

Smith AT, Williams AL, Singh KD (2004): Negative BOLD in the visual cortex: Evidence against blood stealing. Hum Brain Mapp 21:213–220.

Tanabe S, Doi T, Umeda K, Fujita I (2005): Disparity-tuning characteristics of neuronal responses to dynamic random-dot stereograms in macaque visual area V4. J Neurophysiol 94: 2683–2699.

Teo PC, Sapiro G, Wandell BA (1997): Creating connected representations of cortical gray matter for functional MRI visualization. IEEE Trans Med Imaging 16:852–863.

Tootell RB, Mendola JD, Hadjikhani NK, Liu AK, Dale AM (1998): The representation of the ipsilateral visual field in human cerebral cortex. Proc Natl Acad Sci U S Am 95:818–824.

Van de Moortele PF, Auerbach EJ, Olman C, Yacoub E, Uğurbil K, Moeller S (2009): T1 weighted brain images at 7 Tesla unbiased for proton density, T2* contrast and RF coil receive B 1 sensitivity with simultaneous vessel visualization. Neuroimage 46:432–446.

Victor JD, Apkarian P, Hirsch J, Conte MM, Packard M, Relkin NR, Kim KH, Shapley RM (2000): Visual function and brain organization in non-decussating retinal-fugal fibre syndrome. Cereb Cortex 10:2–22.

VISTA. VISTA Stanford vision and imaging science and technology: https://www.stanford.edu/group/vista/cgi-bin/home/software.

von dem Hagen EA, Houston GC, Hoffmann MB, Morland AB (2007): Pigmentation predicts the shift in the line of decussation in humans with albinism. Eur J Neurosci 25:503–511.

von dem Hagen EA, Hoffmann MB, Morland AB (2008): Identifying human albinism: a comparison of VEP and fMRI. Invest Ophthalmol Vis Sci 49:238–249.

Wade AR, Brewer AA, Rieger JW, Wandell BA (2002): Functional measurements of human ventral occipital cortex: retinotopy and colour. Philos Trans R Soc London 357:963–973.

Wandell BA, Chial S, Backus BT (2000): Visualization and measurement of the cortical surface. J Cogn Neurosci 12:739–752.

Wandell BA, Dumoulin SO, Brewer AA (2007): Visual field maps in human cortex. Neuron 56:366–383.

Winawer J, Horiguchi H, Sayres RA, Amano K, Wandell BA (2010): Mapping hV4 and ventral occipital cortex: the venous eclipse. J Vis 10:1.

Wolynski B, Kanowski M, Meltendorf S, Behrens-Baumann W, Hoffmann MB (2010): Self-organisation in the human visual system—Visuo-motor processing with congenitally abnormal V1 input. Neuropsychologia 48:3834–3845.

Zaitsev M, Hennig J, Speck O (2004): Point spread function mapping with parallel imaging techniques and high acceleration factors: Fast, robust, and flexible method for echo-planar imaging distortion correction. Magn Reson Med 52:1156–1166.